



OPEN

Optical twin-vortex multi-trapping by Kolakoski lenses

Arlen B. Perez-Hernández¹, Adrián Garmendia-Martínez¹, Walter D. Furlan²,
 Juan C. Castro-Palacio¹, Juan A. Monsoriu¹ & Francisco M. Muñoz-Pérez^{1,3}✉

In this work, we design and implement a new bifocal diffractive spiral lens within an optical tweezers system. The proposed diffractive optical element coined Kolakoski Kinoform Spiral Lens (KKSL), generates twin optical vortices along the propagation direction. The axial positions, as well as the diameters of the generated vortex beams, are correlated with the Kolakoski aperiodic sequence introduced in the design of the diffractive lens. The unique properties of KKSLs make it ideal for optical trapping applications, allowing independent multiple trapping and particle displacement within each optical vortex beam. We present both the focusing properties of KKSL and the experimental results of its integration into the optical tweezer setup.

In recent decades, optical trapping and manipulation have become a widely used tool, enabling the development of diverse applications in areas such as nanoscience, biophysics, and quantum technologies^{1–3}. This evolution has increased the need to create optical trapping configurations that are tailored to specific needs. Precise control of the optical manipulation of micro- and nanostructures has driven the search for targeted beam-trap design strategies^{4–7}.

One of the widely used trapping systems is optical tweezers, which has proven to be a versatile method for confining particles. However, with the development of new Diffractive Optical Elements (DOEs) for the formation of structured beams and their combination with optical tweezers, it has been shown that it is possible to significantly enhance the functionality of this system^{8,9}. The ability to create phase masks that allow the generation of multiple focal planes, as well as specific intensity structures, translates into the creation of various optical trap configurations¹⁰. An example of this is the ability to transfer angular momentum to the confined particles, displacing them around the optical axis through optical vortices¹¹. Like multifocal diffractive lenses, these features make vortex beams potential tools in optical capture systems by adding a new strategy for particle trapping and manipulation. In this context, the design of DOEs for vortex generation has become relevant in recent years and several proposals can be found in the literature. One of the most common methods for the formation of these structures is the design of spiral phase masks¹². These diffractive elements allow the formation of vortex beams, characterized by a phase singularity and a number called topological charge. These vortex beams exhibit an angular momentum composed of an orbital component coming from the phase and intensity, and a helical phase caused by their azimuthal dependence^{13,14}. The incorporation of DOEs with spiral phase masks into an optical tweezers system has enabled the development of a wide range of applications beyond traditional particle confinement¹⁵. The ability to generate complex beam structures and multiple focal planes has enabled precise control and manipulation of particles in three dimensions^{16–18}.

On the other hand, diffractive lenses based on aperiodic sequences present interesting focusing and imaging^{19–21}. In fact, various aperiodic sequences allow the design of new multifocal diffractive lenses. Examples of these previously employed sequences are Thue-Morse sequence²², Fibonacci sequence²³, m-Bonacci generalization²⁴ and Walsh functions²⁵. Each of these aperiodic sequences provides unique features that translate into specific optical properties for each aperiodic diffractive lens. This is why the possibility of combining this type of lens with spiral phase masks has allowed the generation of DOEs that combine the optical focusing characteristics of both. This has been shown in previous work based on the Fibonacci sequence or inspired by the Cantor fractal^{26,27}. These DOEs generate intensity structures characterized by the formation of multiple axially located vortices, which is functional in the formation of volumetric optical traps and particle manipulation. Although previous research has suggested the possible application of twin vortex-generating diffractive elements in the field of optical trapping, such as the case reported in the literature using the Fibonacci sequence²⁸, these claims have not been experimentally demonstrated. In contrast to these studies, this manuscript aims to experimentally showcase the potential of these elements for application in optical trapping and manipulation. To achieve this, we propose the design of a Kinoform-structured diffractive lens based on the Kolakoski aperiodic

¹Centro de Tecnologías Físicas, Universitat Politècnica de València, 46022 Valencia, Spain. ²Departamento de Óptica y Optometría y Ciencias de la Visión, Universitat de Valencia, 46100 Valencia, Spain. ³Institut Universitari de Ciència dels Materials (ICMUV), Universitat de València, 46100 Burjassot, Spain. ✉email: francisco.m.munoz@uv.es

sequence, which enhances diffractive efficiency by directing energy primarily to a single diffraction order. In addition to the experimental demonstration, the proposed diffractive lens design offers a distinct feature compared to the existing literature. By doing so, we aim to validate the capability of twin vortices to interact with particles in the context of optical manipulation, providing a stronger foundation for future technological applications in this field. Another relevant feature that aperiodic diffractive lenses bring to this scenario is the generation of multiple traps and the control of their axial position through the order of the design sequence²⁹. Some examples of this can be found in the literature, highlighting diffractive lenses based on Silver Mean or m-Bonacci aperiodic sequences, which, when implemented in an optical tweezers system, incorporate a digital position control through the order of the sequence^{24,30}. Unlike DOEs that allow the generation of vortices and thus the transfer of angular momentum to confined particles, diffractive lenses based on aperiodic sequences such as those mentioned above only create point optical traps.

Recently, we presented a new bifocal lens based on the Kolakoski sequence, called the Kolakoski Zonal Plate³¹. This amplitude binary lens generates a pair of axially shaped foci, whose relationship between the two planes can be controlled by the order of the aperiodic Kolakoski sequence. Due to its binary nature of amplitude, the intensity distribution is spread among the different diffraction orders, which reduces its diffractive efficiency. To improve this, we propose a new Kinoform-type design, thus increasing its efficiency for optical trapping applications. In this paper we also introduce the design of a new DOE, the Kinoform Kolakoski Spiral Lens (KKSL), and its implementation in an experimental optical tweezers setup. The KKSL allows the formation of two twin vortices on the axial axis, being the distance between them related with the aperiodic sequence. The diameter of both vortices is determined by a single topological charge, with one of them being twice the diameter of its twin. The intrinsic characteristics of the KKSL make it ideal as an optical trapping system, allowing multiple trapping of particles in each vortex and generating independent displacement dynamics. The focusing properties of the lens are presented, a comparison is made with its binary amplitude counterpart, and experimental results of its application in the assembly of optical tweezers are exhibited.

Kinoform Kolakoski Lens design

The KKLS considered in this work are blazed DOEs whose phase distribution is based on the binary aperiodic Kolakoski sequence. The Kolakoski sequence³² is an aperiodic sequence, which is identical to its own run-length sequence. In Mathematics, the so-called “run-length sequence” of a given sequence is itself the sequence formed by those positive integers that indicate the number of elements of equal consecutive symbols in the sequence. Starting from a seed $K_1 = \{1, 2\}$, we can generate higher orders of this sequence K_S from the previous one, K_{S-1} , by applying the substitution rule to the j -th element of K_{S-1} in the flowing way: $1 \rightarrow 1$ and $2 \rightarrow 11$ if j is an odd number and $1 \rightarrow 2$ and $2 \rightarrow 22$ if j is an even number. Therefore, $K_2 = \{1, 2, 2\}$, $K_3 = \{1, 2, 2, 1, 1\}$, $K_4 = \{1, 2, 2, 1, 1, 2, 1\}$, $K_5 = \{1, 2, 2, 1, 1, 2, 1, 2, 2, 1\}$, $K_6 = \{1, 2, 2, 1, 1, 2, 1, 2, 2, 1, 2, 2, 1\}$, ... Note that the run-length sequence of K_S is K_{S-1} . The total number of elements of the sequence K_S grow exponentially, $L_S = 2, 3, 5, 7, 10, 15, 23, 34, \dots$ and can be approximated to $L_S \approx 2 \cdot \varphi^{S-1}$ where φ is the ratio between the lengths of two consecutive Kolakoski sequences³¹

$$\varphi = \lim_{S \rightarrow \infty} \frac{L_S}{L_{S-1}} = 3/2. \quad (1)$$

The Kolakoski sequence was previously used to design a binary phase zone plate³¹. Fig. 1a) shows the construction of the KZP phase profile of order $S = 8$ from the corresponding Kolakoski sequence in the normalized squared radial coordinate $\zeta = (r/a)^2$, where r is the radial coordinate and a is the lens radius. The corresponding sequence, K_S , is used to define the binary phase distribution, $\Phi_S(\zeta)$ in the compact interval $\zeta \in [0, 1]$. This interval is divided in L_S intervals of length $d_S = 1/L_S$. The associated phase of the j -th subinterval is $\Phi_{S,j} = \pi K_{S,j}$, so $\Phi_{S,j} = \pi$ rad when the element $K_{S,j} = 1$ and $\Phi_{S,j} = 0$ rad when $K_{S,j} = 2$. Then, applying symmetry of revolution around the optical axis, we obtain the phase distribution of the lens (see Fig. 1b)). In order to improve the diffraction efficiency, here we propose a new kinoform-type design. We define the new phase distribution, $\Phi_S(\zeta)$, of each pair of sub-intervals $\{K_{S,j}, K_{S,j+1}\} = \{2, 1\}$ as a linear variation between $\Phi_S = 0$ rad and $\Phi_S = 2\pi$ rad, otherwise $\Phi_S(\zeta) = 0$ rad. In mathematical terms, the generating function of the radial phase for the S -th order KKL can be written as,

$$\Phi_S(\zeta) = \frac{2\pi}{2d_S} \sum_{j=1}^{L_S-1} \text{rect} \left[\frac{\zeta - j d_S}{2d_S} \right] (\zeta - d_S(j-1)) \delta_{2,K_{S,j}} \delta_{1,K_{S,j+1}}. \quad (2)$$

Fig. 1c) shows the phase distribution along ζ of KKL of order $S = 8$. In the same way as the KZP, the KKL can be generated by applying symmetry of revolution around the optical axis (see Fig. 1d)).

Focusing properties of KKLS

To assess the focusing characteristics of KKLS, we have calculated the axial irradiance under monochromatic plane wave illumination using the Fresnel approximation³³

$$I(u) = 4\pi u^2 \left| \int_0^1 t(\zeta) \exp(-i2\pi u \zeta) d\zeta \right|^2, \quad (3)$$

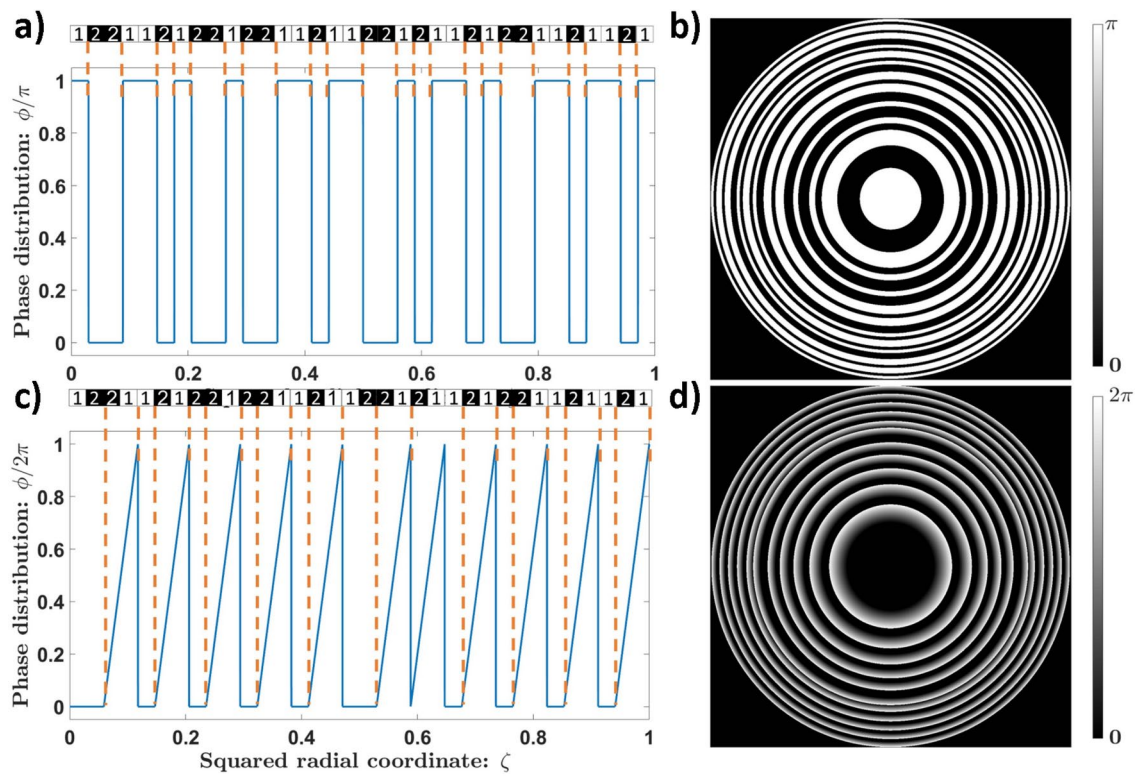


Figure 1. Design of a KZP and KKL of order $S = 8$. (a) Phase profile of the binary KZP represented in the normalized square radial coordinate and (b) the associated pupil phase distribution where white and black regions correspond to phase π and 0, respectively. (c) the Phase profile of the KKL in the normalized square radial coordinate, and (d) the associated pupil phase distribution.

where $u = a^2/2\lambda z$ is the reduced axial coordinate, λ is the wavelength of the incident light, z is the axial distance, and $t(\zeta) = \exp[i\Phi_S(\zeta)]$ is the transmittance function, being $\Phi_S(\zeta)$ the phase function of the lens. By using Eq. 3, we have obtained the axial irradiances provided by KKLs of orders $S = 8$ and $S = 9$ and, for comparison, porpoises those corresponding to binary KZPs of the same orders. The results are shown in Fig. 2. The axial irradiances have been normalized with respect to the maximum value achieved by KKLs. As can be seen, KKLs drive most of the incoming light into the first diffraction order, whereas KZPs present higher diffraction orders due to the binary nature of their structure. The KKLs maintain the bifocal behavior from the KZPs providing two single foci of similar intensity located at $u_a \approx 2\varphi^{S-1}/3 \approx 11.3$ and $u_b \approx 4\varphi^{S-1}/3 \approx 22.7$ for the KKL of order $S = 8$, and $u_a \approx 2\varphi^{S-1}/3 \approx 16.6$ and $u_b \approx 4\varphi^{S-1}/3 \approx 33.1$ for the KKL of order $S = 9$. The relative intensities provided by the KZPs at the foci are 60% lower compared to those provided by KKLs, thus this new kinoform design improves the diffraction efficiency of this DOE extending its suitability to different optical applications.

Design and focusing properties of Kinoform Kolakoski spiral lenses

A Kinoform Kolakoski Spiral Lens (KKSL) is defined as a pure phase diffractive element whose phase distribution is given by

$$\Phi_{KKSL}(\theta, \zeta) = \text{mod}_{2\pi}[m\theta + \Phi_S(\zeta)]. \quad (4)$$

It combines the azimuthal phase variation that characterizes a vortex lens, where m is a non-zero integer called the topological charge³⁴ and θ is the azimuthal angle about the optical axis at the pupil plane, with the radial phase distribution of a KKL given by Eq. 2. Thus a KKSL with $m = 0$ can be understood as a KKL. Fig. 3 shows two KKSLs based on the Kolakoski sequence of order $S = 8$ with topological charges $m = 3$ and $m = 6$.

We calculated the irradiance distribution provided by the lenses shown in Fig. 3 when illuminated by a plane wave with wavelength λ in a specific volume. Within the Fresnel approximation, the irradiance function is given by

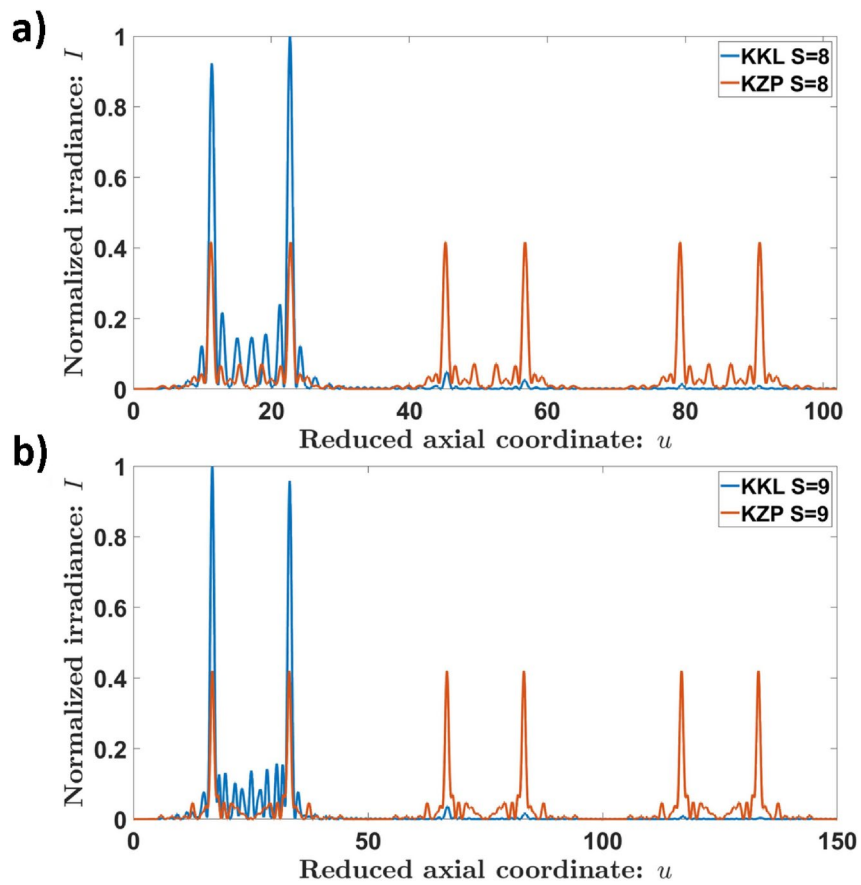


Figure 2. Axial irradiance distributions along the reduced axial coordinate produced by the KKLs and the KZPs of orders (a) $S = 8$ and (b) $S = 9$.

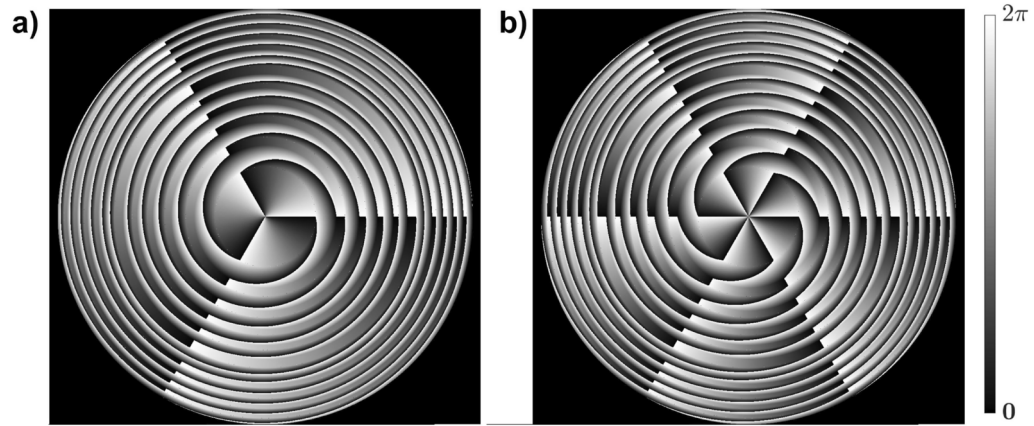


Figure 3. Phase distributions of KKSLs of order $S = 8$ with topological charges (a) $m = 3$ and (b) $m = 6$.

$$I(\bar{x}, \bar{y}, u) = u^2 \left| \int_{-1}^1 \int_{-1}^1 t_{KKSL}(\bar{x}_0, \bar{y}_0) e^{i2\pi u(\bar{x}_0^2 + \bar{y}_0^2)} e^{-i2\pi 2u(\bar{x}\bar{x}_0 + \bar{y}\bar{y}_0)} d\bar{x}_0 d\bar{y}_0 \right|^2, \quad (5)$$

where $\bar{x} = x/a$ and $\bar{y} = y/a$ denote the normalized transversal coordinates, $\bar{x}_0 = x_0/a$ and $\bar{y}_0 = y_0/a$ are the normalized transversal coordinates in the pupil plane, and $t_{KKSL}(\bar{x}_0, \bar{y}_0) = \exp[i\Phi_{KKSL}(\bar{x}_0, \bar{y}_0)]$ is the transmittance function whose phase distribution is defined by Eq.4 after performing the variable changes $\zeta = \bar{x}_0^2 + \bar{y}_0^2$ and $\theta = \arctan(\bar{y}_0/\bar{x}_0)$. The integrals were solved numerically by applying the 2D Fast Fourier Transform method³³.

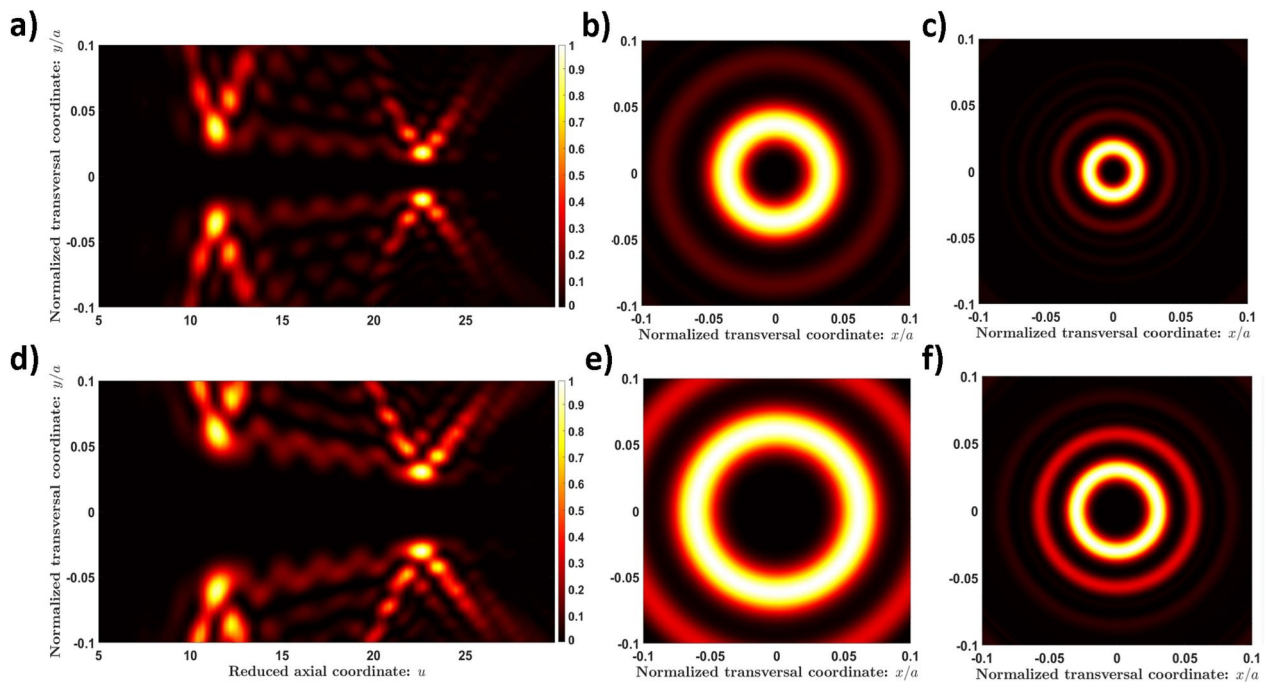


Figure 4. Evolutions of the transversal irradiances for KKSLs of order $S = 8$ with topological charges, **(a)** $m = 3$ and **(d)** $m = 6$. Irradiance distributions are provided by both lenses at the focal planes, **(b, e)** $u = u_a$ and **(c, f)** $u = u_b$.

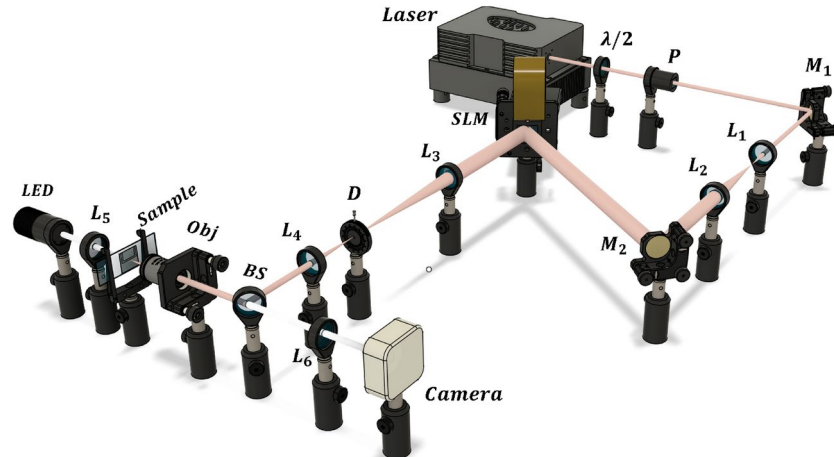


Figure 5. Experimental setup for particle trapping and manipulation utilizing KKSL-based optical tweezers.

Fig. 4a) and 4d) show the irradiance distributions in the zx plane provided by the KKSLs of order $S = 8$ with topological charges $m = 3$ and $m = 6$, respectively. Both lenses produce a pair of doughnut-shaped foci, the positions of which are the same as the focal distances of the KKLs of the same order: $u_a \approx 2\varphi^{S-1}/3 \approx 11.3$ and $u_b \approx 4\varphi^{S-1}/3 \approx 22.7$. The ratio between the positions where these vortices are located is approximately 2. Thus, the KKSLs maintain the focusing properties inherent to the aperiodic sequence on which they are based. The irradiance distributions at each of the foci planes, $u = u_a$ and $u = u_b$, are shown in Fig. 4b), 4c), 4e), 4f) for both lenses. Comparing these patterns, it can be verified that the diameter of the vortex increases with the topological charge.

Experimental results

We have developed an optical tweezers setup to demonstrate the multi-trapping capabilities of KKSL, as shown in Fig. 5. A beam CW laser ($\lambda = 1064$ nm, Laser Quantum, Mod. Opus 1064) with a maximum power output of 3 W, passes through a half-wave plate ($\lambda/2$), followed by a linear polarizer (P) to adjust the beam's linear

polarization direction. The beam is then redirected by mirrors (M_1 and M_2) and expanded using a magnification system with a factor of 3x, consisting of lenses L_1 and L_2 ($f_1 = 50$ mm and $f_2 = 150$ mm). The KKSL is projected onto a spatial light modulator (SLM) (Holoeye PLUTO-2.1-NIR-149, phase type, pixel size 8 μm , resolution 1920 x 1080 pixels), configured to achieve a phase shift of 2.1π for a wavelength of 1064 nm. The modulated KKSL beam is steered through a 4f system consisting of lenses L_3 ($f_3 = 150$ mm) and L_4 ($f_4 = 150$ mm). A 1D blazed grating is incorporated into each KKSL to serve as a linear phase carrier. This design directs the diffracted light towards the first order of diffraction, effectively eliminating noise from specular reflections in higher diffraction orders. A diaphragm (D) at the focal point of L_3 performs spatial filtering, allowing only the first-order diffraction to pass. By slightly tilting the SLM, the linear phase carrier aligns the first-order diffraction with the diaphragm optical axis.

As shown in Fig. 5, the KKSL image passes through a high-numerical-aperture oil-immersion objective (Olympus UPLFLN 100X, NA = 1.3) located at the focal plane of L_4 . An LED light source (Thorlabs, Mounted High-Power, 1300 mA, Mod. MCWHL7) is used to illuminate the sample. The LED light is collimated and then focused onto the sample using the L_5 lens ($f_5 = 30$ mm). A beam splitter (BS) transmits visible light from the sample while blocking infrared reflections from the imaging system. Finally, the L_6 lens ($f_6 = 50$ mm) focuses the image, which is then captured by a CMOS camera sensor (Edmund Optics, Mod. EO-10012C) in this optical setup.

Next, we analyze experimental results demonstrating the trapping and manipulation of microparticles in each vortex located in the focal planes generated by a KKSL. Fig. 6 a) - c) shows the stable trapping of polystyrene microparticles (diameter $\approx 2\mu\text{m}$) using a KKSL of order $S = 8$ and topological charge $m = -14$. The microparticles, interacting with the vortices, are confined and experience displacement dynamics over the profile of each ring. Fig. 6 indicates the rotational motion with an arrow pointing to the direction of rotation. To illustrate this behavior, an individual particle in each vortex has been selected, marking its motion with a red dot for the particle confined in the largest diameter vortex and an orange dot for the one in the second vortex.

As predicted theoretically, the formation of two focal planes and the generation of a vortex in each by the KKSL allow for the multiple capture of microparticles (see Video 1). Through the order S , a functional relationship is established between the two foci, and by means of the parameter m , the diameter of the vortices can be manipulated. That is, as m increases, the diameter of both vortices also increases. It is observed that the vortices have different diameters, with an approximate ratio of $D_2 \approx 2D_1$, a property related to the Kolakoski aperiodic sequence (see Fig. 6 a)). Furthermore, the direction of rotation for both vortices is determined by the sign of m . When dealing with negative topological charges, the rotation direction is counterclockwise; conversely, for positive charges, it is clockwise. The design characteristics of the KKSL, such as its Kinoform structure and its focusing properties reflected in the generation of twin vortices, offer an alternative for the formation of volumetric optical traps. The dynamics of the vortices, by imparting angular momentum, along with the multiple particle trapping along each vortex, add new control capabilities to the optical tweezers system, thanks to the order of the Kolakoski sequence and the topological charge implicit in the phase mask design. The experimental demonstration of the use of twin vortex-generating diffractive elements as optical traps, reported for the first time, will pave the way for new applications, such as the creation of micromachines, among others.

Conclusion

We have designed and implemented an optical tweezers system based on KKSL, aimed at trapping multiple particles in the vortices generated along the optical axis. These lenses create two main foci, with a focal length ratio related to the order parameter of the Kolakoski sequence. At each focal point, a vortex is generated, where confined particles move along the circumference due to the angular momentum imparted by the phase distribution. Through a topological charger, it is possible to adjust the diameter of each vortex, maintaining a size ratio with double the diameter between them.

KKSLs present an innovative approach to three-dimensional manipulation using optical configurations with dynamic trapping control. Optical tweezers that employ holographic techniques are expanding into new applications across various fields. The development of KKSLs has the potential to address limitations in optical

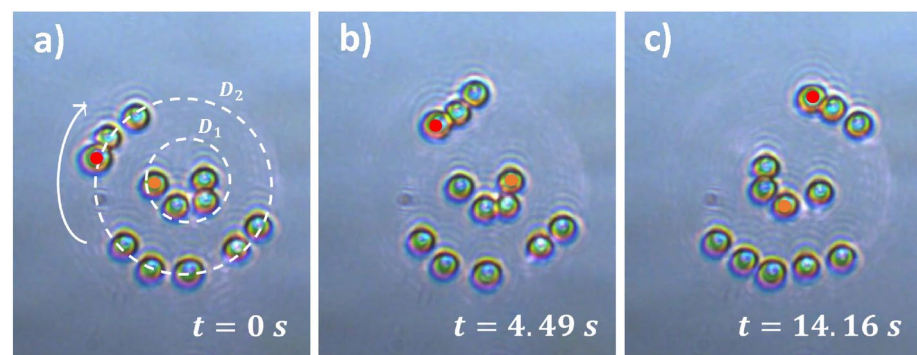


Figure 6. Image sequences of particles multi-trapping and manipulation by KKSL-based optical tweezers.

trapping and longitudinal confinement. We expect these lenses to play a vital role, particularly in microrobots, enabling nanoscale mechanical operations for microvalves, micromotors, and precise microassembly.

Data availability

All data generated or analysed during this study are included in this published article.

Received: 11 September 2024; Accepted: 23 October 2024

Published online: 05 November 2024

References

1. Hu, S., Liao, Z., Cai, L. & Jiang, X. Near-field optical tweezers for chemistry and biology. *Phys. Status Solidi A* **217**, 1900604 (2020).
2. Bustamante, C. J., Chemla, Y. R., Liu, S. & Wang, M. D. Optical tweezers in single-molecule biophysics. *Nature Reviews Methods Primers* **1** (2021).
3. Kaufman, A. & Ni, K. Quantum science with optical tweezer arrays of ultracold atoms and molecules. *Nat. Phys.* **17**, 1324–1333 (2021).
4. Arias-Gonzalez, J. R. Optical tweezers to study viruses. *Subcell. Biochem.* **68**, 273–304 (2013).
5. Stoev, I., Seelbinder, B., Erben, E. & et al. Highly sensitive force measurements in an optically generated, harmonic hydrodynamic trap. *eLight* **1** (2021).
6. Rodríguez-Rodríguez, H., Salas, G. & Arias-Gonzalez, J. R. Heat generation in single magnetic nanoparticles under near-infrared irradiation. *J. Phys. Chem. Lett.* **11**, 2182–2187 (2020).
7. Balushi, A. A. A. et al. Label-free free-solution nanoaperture optical tweezers for single molecule protein studies. *Analyst* **140**, 4760–4778 (2015).
8. Gahagan, K. & Jr., G. S. Optical vortex trapping of particles. *Opt. Lett.* **21** (1996).
9. Lee, W., Yuan, X.-C. & Cheong, W. Optical vortex beam shaping by use of highly efficient irregular spiral phase plates for optical micromanipulation. *Opt. Lett.* **29** (2004).
10. Cheng, S., Zhang, X., Ma, W. & Tao, S. Fractal zone plate beam based optical tweezers. *Sci. Rep.* **6** (2016).
11. Tian, Y., Wang, L., Duan, G. & Yu, L. Multi-trap optical tweezers based on composite vortex beams. *Optics Communications* **485**, 126712 (2021).
12. Machado, F., Zagrajek, P., Ferrando, V., Monsoriu, J. A. & Furlan, W. D. Multiplexing THz vortex beams with a single diffractive 3-d printed lens. *IEEE Trans. Terahertz Sci. Technol.* **9**, 63–66 (2019).
13. Schmitz, K., C. H. J. and Uhrig, Spatz, J. P. & Curtis, J. E. Tuning the orbital angular momentum in optical vortex beams. *Opt. Express* **14**, 6604–6612 (2006).
14. Roux, F. S. Distribution of angular momentum and vortex morphology in optical beams. *Opt. Commun.* **242**, 45–55 (2004).
15. Muñoz-Pérez, F. M. et al. Multiplexed vortex beam-based optical tweezers generated with spiral phase mask. *iScience* **26**, 107987 (2023).
16. Gecevičius, M., Drevinskasa, R., Beresna, M. & Kazansky, P. G. Single beam optical vortex tweezers with tunable orbital angular momentum. *Appl. Phys. Lett.* **104**, 231110 (2014).
17. Padgett, M. & Bowman, R. Tweezers with a twist. *Nat. Photonics* **5**, 343–348 (2011).
18. Liang, Y. et al. Rotating of low-refractive-index microparticles with a quasi-perfect optical vortex. *Appl. Opt.* **57**, 79–84 (2018).
19. Saavedra, G., Furlan, W. D. & Monsoriu, J. A. Fractal zone plates. *Opt. Lett.* **28**, 971–973 (2003).
20. Furlan, W. D., Saavedra, G. & Monsoriu, J. A. White-light imaging with fractal zone plates. *Opt. Lett.* **32**(15), 2109–2111 (2007).
21. Giménez, F., Furlan, W. D., Calatayud, A. & Monsoriu, J. A. Multifractal zone plates. *J. Opt. Soc. Am. A* **27**, 1851–1855 (2010).
22. Ferrando, V., Giménez, F., Furlan, W. D. & Monsoriu, J. A. Bifractal focusing and imaging properties of thue-morse zone plates. *Opt. Express* **23**(15), 19846–19853 (2015).
23. Monsoriu, J. A. et al. Bifocal fibonacci diffractive lenses. *IEEE Photonics J.* **5**(3), 3400106 (2013).
24. Muoz-Pérez, F. M., Ferrando, V., Furlan, W. D., Monsoriu, J. A. & Arias-Gonzalez, J. R. Optical multi-trapping by kinoform m-bonacci lenses. *Opt. Express* **30**, 34378–34384 (2022).
25. Machado, F., Ferrando, V., Giménez, F., Furlan, W. D. & Monsoriu, J. A. Multiple-plane image formation by walsh zone plates. *Opt. Express* **26**(16), 21210–21218 (2018).
26. Calatayud, A. et al. Experimental generation and characterization of devil's vortex-lenses. *Appl. Phys. B* **106**, 915–919 (2012).
27. Furlan, W., Giménez, F., Calatayud, A. & Monsoriu, J. Devils vortex-lenses. *Opt. Express* **17**, 21819–21896 (2009).
28. Calatayud, A., Ferrando, V. & and, F. G. Twin axial vortices generated by fibonacci lenses. *Opt. Express* **21**, 10234–10239 (2013).
29. Liang, Y. et al. Simultaneous optical trapping and imaging in the axial plane: a review of current progress. *Rep. Prog. Phys.* **83** (2020).
30. Muñoz-Pérez, F. M. et al. Multi-trap optical tweezers based on kinoform silver mean lenses. *Optik* **311**, 171913 (2024).
31. Garmendia-Martínez, A., Muñoz-Pérez, F. M., Furlan, W. D., Ferrando, V. & Monsoriu, J. A. Bifocal diffractive lenses based on the aperiodic kolakoski sequence. *Sci. Rep.* **14**, 14249 (2024).
32. Sing, B. Kolakoski sequences - an example of aperiodic order. *Journal of Non-Crystalline Solids* **334–335**, 100–104 (2004). 8th International Conference on Quasicrystals.
33. Garmendia-Martínez, A. et al. Comparative study of numerical methods for solving the fresnel integral in aperiodic diffractive lenses. *Mathematics* **11** (2023).
34. Dai, H. T., Liu, Y. J. & Sun, X. W. The focusing property of the spiral Fibonacci zone plate. In Jiang, S., Digonnet, M. J. F. & Dries, J. C. (eds.) *Optical Components and Materials IX*, vol. 8257, 82570T. International Society for Optics and Photonics (SPIE, 2012).

Acknowledgements

This work was supported by the Spanish Ministerio de Ciencia e Innovación (grant PID2022-142407NB-I00) and by Generalitat Valenciana (grant CIPROM/2022/30), Spain. A.G.M. and A.B.P. acknowledge the financial support from the Generalitat Valenciana (GRISOLIAP/2021/121) and Universitat Politècnica de València (PAID-01-23), respectively.

Author contributions

A.P., A.G., W.F., V.F., and J.M. conceived the experiments, A.G., F.M., and V.F. conducted the experiments, and A.G., V.F., F.M., and J.M. analyzed the results. All authors reviewed the manuscript.

Additional information

Supplementary Information The online version contains supplementary material available at <https://doi.org/10.1038/s41598-024-77596-z>

[0.1038/s41598-024-77596-z](https://doi.org/10.1038/s41598-024-77596-z).

Correspondence and requests for materials should be addressed to F.M.M.-P.

Reprints and permissions information is available at www.nature.com/reprints.

Publisher's note Springer Nature remains neutral with regard to jurisdictional claims in published maps and institutional affiliations.

Open Access This article is licensed under a Creative Commons Attribution-NonCommercial-NoDerivatives 4.0 International License, which permits any non-commercial use, sharing, distribution and reproduction in any medium or format, as long as you give appropriate credit to the original author(s) and the source, provide a link to the Creative Commons licence, and indicate if you modified the licensed material. You do not have permission under this licence to share adapted material derived from this article or parts of it. The images or other third party material in this article are included in the article's Creative Commons licence, unless indicated otherwise in a credit line to the material. If material is not included in the article's Creative Commons licence and your intended use is not permitted by statutory regulation or exceeds the permitted use, you will need to obtain permission directly from the copyright holder. To view a copy of this licence, visit <http://creativecommons.org/licenses/by-nc-nd/4.0/>.

© The Author(s) 2024